SUPPLEMENTAL MATERIALS AND METHODS

Generation of MEFs, osteoblasts and cell culture

Prkar1a$^{-/-}$ and control MEFs were generated and cultured as described (Nadella and Kirschner, 2005). Briefly, parallel MEF cultures were isolated from single littermate embryos and genotyped. *Prkar1a*$^{+/+}$ *and Prkar1a*$^{loxP/loxP}$ MEFs were treated with retroviral cre to produce Prkar1a(WT) and Prkar1a(KO) lines, respectively. Tumor and normal osteoblasts from tail tumors of *Prkar1a*$^{+/-}$ and wild type mice were prepared and cultured as described (Pavel et al., 2008). All cells were routinely cultured in Dulbecco's modified Eagle's medium with 10% fetal bovine serum.

Cell migration

Cell migration was performed as described (Saji et al., 2005). Briefly, cells were collected in DMEM/0.2% FBS and adjusted to 10^5/ml for WT and 8L and 2 x 10^5/ml for 2L and 300 µL of the cell suspension were seeded in upper chamber of a Boyden Chamber. After 1 hour, cells were stimulated to migrate by placement in wells containing DMEM/5%. After 6 hours of migration, the reaction was terminated and the samples quantitated as described. PKI treatment (10 uM) included a 30 min pre-treatment and fresh drug during the migration period. The basal migration experiments were repeated 4-6 times each, and the PKI studies were repeated 3-4 times each.

Wound-healing assays

Wound-healing assays were performed with the ECIS 1600R (Applied BioPhysics, Troy, NY). For these studies, 40,000 cells were cultured on ECIS eight-well culture dish (ECIS

8W1E plate). After the cells were grown to confluence, the cells are subjected to an elevated voltage pulse of 40-kHz frequency, 3.5-V amplitude, and 30-s duration, which led to death and detachment of cells present on the small active electrode, resulting in a wound normally healed by cells surrounding the small active electrode that have not been submitted to the elevated voltage pulse. Wound healing was then assessed by continuous resistance measurements for 48h. The migration abilities of three different Prkar1a knock out MEFs were compared to the wild type MEFs obtained from the same litter.

Statistical Analysis

All analysis was performed by using GB-STAT (Dynamic Microsystems, Inc., Silver Spring, MD). Percent migration was analyzed by ANOVA and significance was analyzed by using Bonferroni/Dunn's methods.

Nadella et al., 2008

Supplementary Table 1
Phylogenetic conservation of PKA phosphorylation sites in Limk1 and Limk2

```
                                    323
                                     |
Hs LIMK1[1]       rspgagslgspasqrkdlgrseslrvv.crphrifrpsdlihgevlgkgcfgqaikv
Mm Limk1          tspgtsslaspasqrkdlgrseslrvv.crphrifrpsdlihgevlgkgcfgqaikv
Pt Limk1          rspgagslgspasqrkdlgrseslrvv.crphrifrpsdlihgevlgkgcfgqaikv
Rn Limk1          tspgagslvspasqrkdlgrseslrvv.crphrifrpsdlihgevlgkgcfgqaikv
Gg Limk1          kspgsssvgspasqrkdigrseslrvv.srahrifrpsdlihgevlgkgcfgqaikv
Dr Limk1          kspssssapsplslrkdigrseslrgvsnrthrifrasdlihgevlgtgcfgqaikv
Dm Limk           deqhqaqqhsahpqlydlsrtqscrvv.qkpqrifratdlvigeklgegffgkvfkv

Hs Limk2          kspgpsspkepllfsrdisrseslrcsssysqqifrpcdlihgevlgkgffgqaikv
Mm Limk2          kspgpsspkeplllsrdisrseslrcsssysqqifrpcdlihgevlgkgffgqaikv
Rn Limk2          kspgpsspkeplllsrdisrseslrcsssysqqifrpcdlihgevlgkgffgqaikv
Gg limk2          kspgpsspkeplllsrdisrseslrsssscsqqifrpcdlihgevlgkgffgqaikv
Dr Limk2          kspvssspkdhlvltrdigrseslrspsscshrifrpcdlihgeilgkgffgqaikv


                                                          596
                                                           |
Hs LIMK1          prtmdfglnvrgfldrycppncppsffpitvrccdldpekrpsfvklehwletl
Mm Limk1          prtmdfglnvrgfldrycppncppsffpitvrccdldpekrpsfvkleqwletl
Pt Limk1          prtmdfglnvrgfldrycppncppsffpitvrccdldpekrpsfvklehwletl
Rn Limk1          prtmdfglnvrgfldrycppncppsffpitvrccdldpekrpsfvkleqwletl
Gg Limk1          prttdfglnvrgflerycppacppsffpiaacccdldpekrpsfskleqwletl
Dr Limk1          praldfglntavfleehcpadcpaaffpiaalccdldaekrpaftkleswledl
Dm Limk           mprnsdfslnqqefrekfcaqcpepfvkvafvccdlnpdmrpcfetlhvwlqrl

Hs Limk2          prtldfglnvklfwekfvptdcppaffplaaiccrlepesrpafskledsfeal
Mm Limk2          prtldfglnvklfwekfvptdcppaffplaaicckepesrpafskledsfeal
Rn Limk2          prtldfglnvklfwekfvptdcppaffplaaicckepesrpafskledsfeal
Gg Limk2          prtldfglnvklfwekfvpadcppaffplaaiccrlepesrppfskledsfeal
Dr Limk2          prtldfglnvrtfiekflpehcppaffalavaccdltpdnrpafqkledcfeal
```

[1] Abbreviations and accession numbers of sequences are as follows:

Abbrev.	Species	Limk1	Limk2
Hs	*Homo sapiens*	NP_002305	NP_001026971
Mm	*Mus musculus*	NP_034847	NP_001029202
Pt	*Pan troglodytes*	XP_001148746	--
Rn	*Rattus norvegicus*	NP_113915	NP_077049
Gg	*Gallus gallus*	NP_989462	NP_990446
Dr	*Danio rerio*	NP_001036156	NP_001002651
Dm	*Drosophila melanogaster*	NP_511139	--

SUPPLEMENTAL FIGURE LEGENDS

Supplemental Figure 1. Loss of Prkar1a enhances cell migration measured by the Electronic Coupled Impedance Sensing (ECIS) assay. a. ECIS analysis of migration of 3 independent *Prkar1a*$^{-/-}$ MEF cell lines compared to WT (*Prkar1a*$^{+/+}$) cells.

Supplemental Figure 2. Enhanced pCofilin and migration are observed in primary cultures of Prkar1a$^{+/-}$ tumor osteoblasts. **a**. Western blotting of pCofilin and Limk1 from primary cultures of normal osteoblasts (N1-4) or 5 independent tumors (T1-5). Actin is shown as a loading control. **b**. ECIS analysis of migration of primary osteoblasts isolated from 3 WT mice and 3 independent *Prkar1a*$^{+/-}$ bone tumors. Note that sample 1 (WT) and sample 5 (Tumor) were not subject to voltage-induced monolayer wounding.

Supplemental Figure 3. PKA activation causes morphologic changes at low cell density. **Left.** WT cells at low density in normal medium. **Middle.** WT cells at low density after 24 hours treatment with 50 uM Forskolin (FSK). **Right.** KO cells at low density. Note the significant number of the cells in the center panel which exhibit the same morphology as KO cells.

Supplemental Figure 4. PKA-C enhances Limk1-mediated phosphorylation of Cofilin. Autoradiogram of *in vitro* kinase assay demonstrating that PKA-C phosphorylates

Limk1 and enhances its ability to phosphorylate of Cofiilin. Note that the background level of Cofilin visualization observed in the first lane is not PKA-C dependent.

Supplemental Figure 5. PKA-C enhances Limk1-mediated phosphorylation of Cofilin *in vivo.* Immunoblot showing the effects of PKA and Limk1 transfected individually or together on Cofilin phosphorylation in intact 293T cells. PTEN is shown as a loading control. Note that the level of pCofilin is much higher in the co-transfected cells than in cells transfected with either kinase by itself.

Supplemental Figure 1 Nadella et al

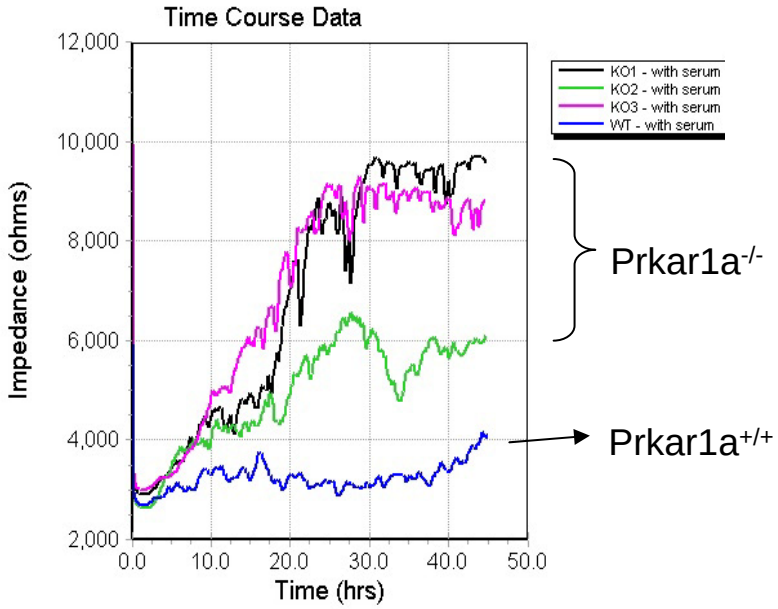

Supplemental Figure 1. Loss of Prkar1a enhances cell migration measured by the Electronic Coupled Impedance Sensing (ECIS) assay. **a.** ECIS analysis of migration of 3 independent *Prkar1a*$^{-/-}$ MEF cell lines compared to WT (*Prkar1a*$^{+/+}$) cells.

Supplemental Figure 2 Nadella et al

a

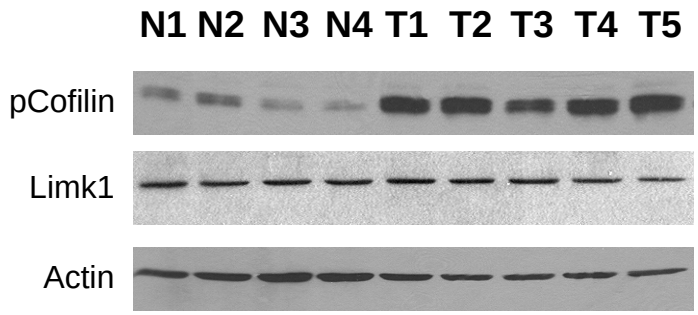

b

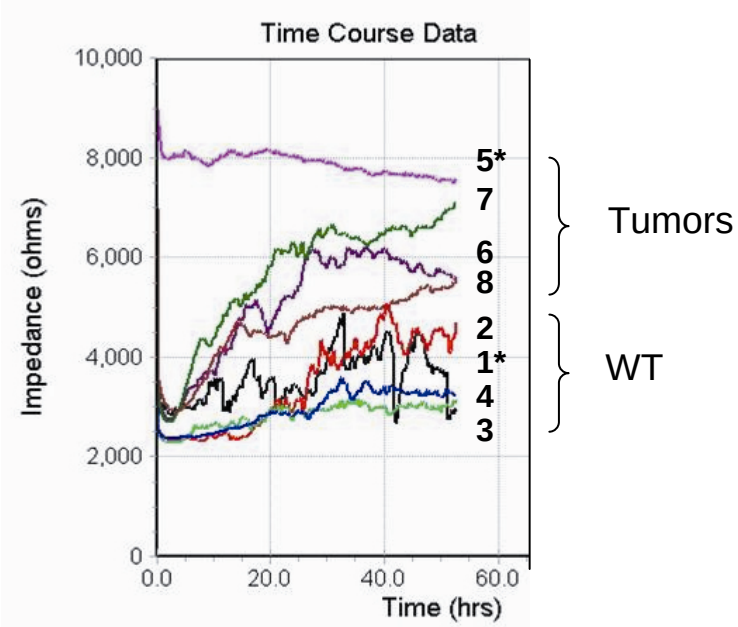

Supplemental Figure 2. Enhanced pCofilin and migration are observed in primary cultures of Prkar1a$^{+/-}$ tumor osteoblasts. **a.** Western blotting of pCofilin and Limk1 from primary cultures of normal osteoblasts (N1-4) or 5 independent tumors (T1-5). Actin is shown as a loading control. **b.** ECIS analysis of migration of primary osteoblasts isolated from 3 WT mice and 3 independent *Prkar1a*$^{+/-}$ bone tumors. Note that sample 1 (WT) and sample 5 (Tumor) were not subject to voltage-induced monolayer wounding.

Supplemental Figure 3 Nadella et al

MEFs

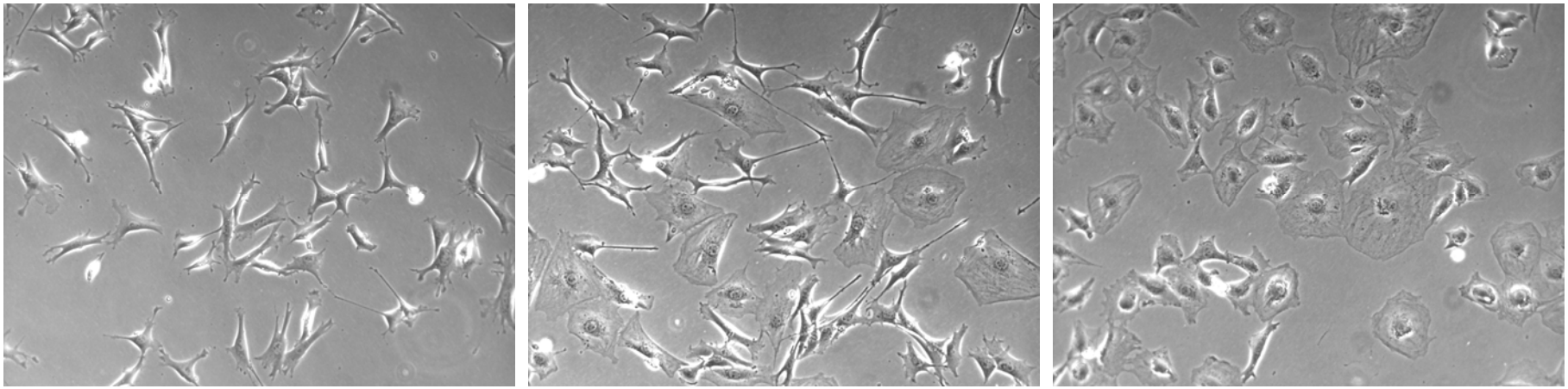

Prkar1a$^{+/+}$ | *Prkar1a*$^{+/+}$ with FSK | *Prkar1a*$^{-/-}$

Supplemental Figure 4 Nadella et al

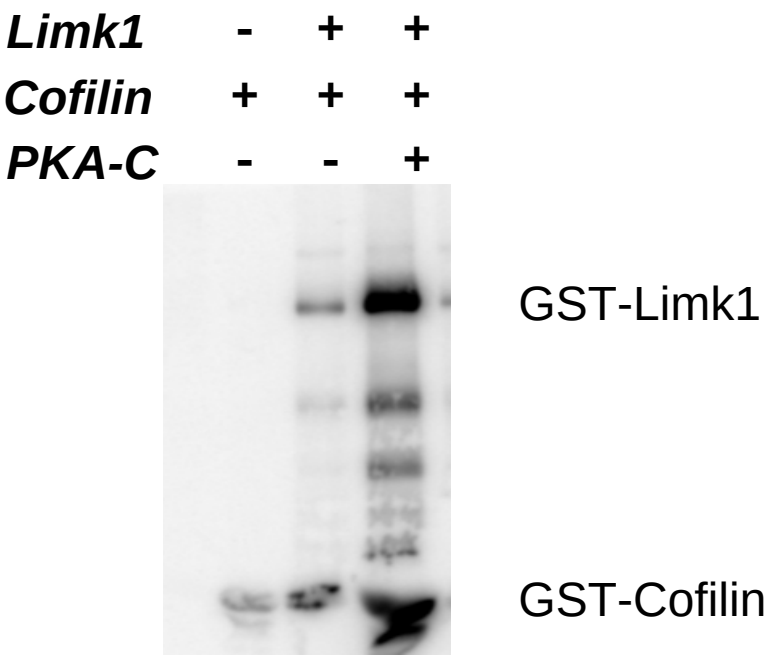

Supplemental Figure 5 Nadella et al